Check for updates

THE AMERICAN SOCIETY OF MECHANICAL ENGINEERS
345 E. 47th St., New York, N.Y. 10017

96-GT-110

The Society shall not be responsible for statements or opinions advanced in papers or discussion at meetings of the Society or of its Divisions or Sections, or printed in its publications. Discussion is printed only if the paper is published in an ASME Journal. Authorization to photocopy material for internal or personal use under circumstance not falling within the fair use provisions of the Copyright Act is granted by ASME to libraries and other users registered with the Copyright Clearance Center (CCC) Transactional Reporting Service provided that the base fee of $0.30 per page is paid directly to the CCC, 27 Congress Street, Salem MA 01970. Requests for special permission or bulk reproduction should be addressed to the ASME Technical Publishing Department.

Copyright © 1996 by ASME All Rights Reserved Printed in U.S.A.

FRICTION DAMPING OF HOLLOW AIRFOILS: PART II – EXPERIMENTAL VERIFICATION

Yehia M. EL–Aini
Chief Engineering
Pratt & Whitney
West Palm Beach, FL 33410–9600

Barry K. Benedict
Materials & Mechanics Engineering
Pratt & Whitney
West Palm Beach, FL 33410–9600

Wen–Te Wu
Department of Mechanical Engineering
Carnegie Mellon University
Pittsburgh, PA 15213

BREAK

ABSTRACT

The use of hollow airfoils in turbomachinery applications, in particular fans and turbines, is an essential element in reducing the overall engine weight. However, state–of–the–art airfoil geometries are of low aspect ratio and exhibit unique characteristics associated with plate–like modes. These modes are characterized by a chordwise form of bending and high modal density within the engine operating speed range. These features combined with the mistuning effects resulting from manufacturing tolerances make accurate frequency and forced response predictions difficult and increase the potential for High Cycle Fatigue (HCF) durability problems. The present paper summarizes the results of an experimental test program on internal damping of hollow blade–like specimens. Friction damping is provided via sheet metal devices configured to fit within a hollow cavity with various levels of preload. The results of the investigation indicate that such devices can provide significant levels of damping provided the damper location and preload is optimized for the modes of concern. The transition of this concept to actual engine hardware would require further optimization with regard to wear effects and loss of preload particularly in applications where the preload is independent of rotational speed. Excellent agreement was achieved between the experimental results and the analytical predictions using a micro–slip friction damping model.

1. INTRODUCTION

Turbomachinery designers have always resorted to the use of passive damping concepts to reduce destructive vibratory responses of engine flowpath components to acceptable limits. The most commonly known approaches are: 1) Dry Friction Dampers, 2) Viscoelastic Dampers, and 3) Impact Dampers. Dry friction dampers are widely used in jet engine applications, particularly in the form of part–span shrouds on fan blades, tip shrouds on low pressure turbine (LPT) blades, and platform dampers on high pressure turbine (HPT) blades. Dry friction dampers are also applied to Labyrinth seals and gears in the form of centrifugally loaded split rings. While design criteria for such dampers has been primarily empirical, recent analysis techniques by Griffin (1980), and Griffin and Menq (1991) have been developed and continue to be the focus of many researchers.

Viscoelastic dampers, although easier to analyze, have infrequently been used by turbomachinery designers in the form of constrained–layer treatment to non–rotating structural members. An example of a successful application of this technique is its use on a Pratt and Whitney TF30 fan inlet guide vane. However, sensitivity to temperature and creep have limited the use of viscoelastic treatments on rotating engine components.

Impact dampers are the least used in engine applications. Analytical design methodologies are nearly non–existent due to the non–linear nature of the problem. Trial and error experiments by Panossian (1989), have demonstrated the benefit of using loose particles in the liquid oxygen (LOX) inlet splitter vane of the Space Shuttle Main Engine (SSME) to reduce the vibratory response to acceptable levels. Validation of this concept on rotating components is yet to be demonstrated.

The continued pursuit of high thrust–to–weight ratio of both military and commercial engine designs has resulted in airfoil designs that are low–aspect–ratio, hollow, and integrally bladed to the disk. The elimination of part–span shrouds and slotted attachments have resulted in lightly damped stages that are susceptible to HCF durability problems. In addition, the use of low–aspect–ratio airfoils has resulted in responses characterized by high modal density of plate–like modes within the engine operating speed range. Therefore, damping augmentation of these new designs has been identified as a critical need.

In this paper, approaches to introduce damping into hollow airfoil–like specimens are examined with emphasis on damping of chordwise flexural modes. Experimental results are summarized and correlated to analytical predictions of a micro–slip friction damping model by Griffin, et al (Part I of this paper).

Presented at the International Gas Turbine and Aeroengine Congress & Exhibition
Birmingham, UK — June 10-13, 1996
This paper has been accepted for publication in the Transactions of the ASME
Discussion of it will be accepted at ASME Headquarters until September 30, 1996

Downloaded from http://asmedigitalcollection.asme.org/GT/proceedings-pdf/GT1996/78767/V005T14A013/4464956/v005t14a013-96-gt-110.pdf by guest on 07 October 2022

2. EXPERIMENTAL PROGRAM

2.1 Hollow Specimens

Three hollow specimens (PW10, PW11, and PW12) were used in this investigation with the main differences being in the thickness of the ribs separating the different hollow regions. The specimens are made of Ti–6–4. Two separately machined halves, with the selected rib pattern shown in Figure 1, are then diffusion bonded together to form the hollow specimen. The cavities at the tip are intentionally left exposed to accept a variety of damper inserts. The specimens are roughly 0.32 inch thick with a skin thickness of 0.062 inch in the airfoil section. The specimens are firmly attached to a fixture using five bolts through the 0.50 inch thick section at the root. To characterize the modal responses of the hollow specimens, both NASTRAN Finite Element modal analyses and laboratory techniques, including holography, impact testing, and Stress Pattern Analysis by Thermal Emission (SPATE) were used to quantify the modes of interest as well as to define the appropriate strain gage locations. Figure 2 is a coarse Finite Element model used to asses the modal characteristics of the specimens. The model is constructed using plate elements to represent the airfoil skins and ribs (shown as dark shaded elements).

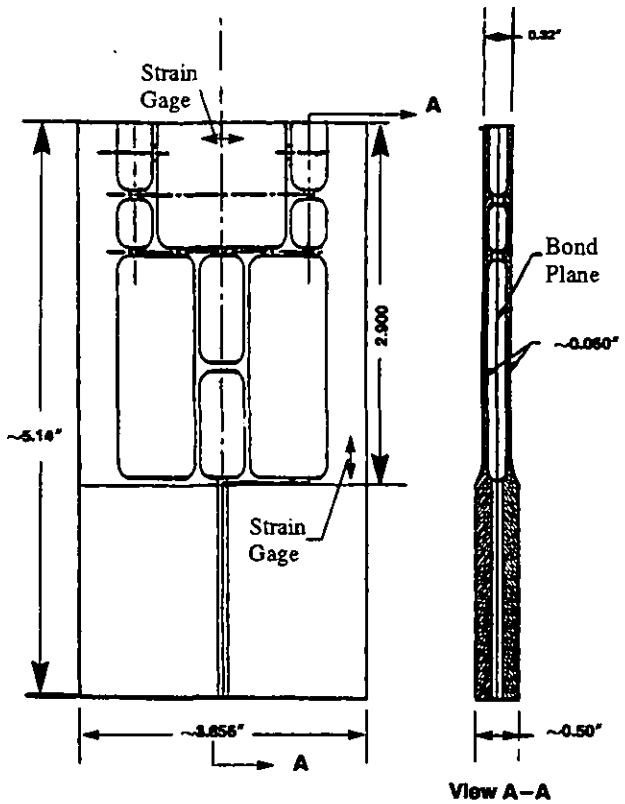

Figure 1: Hollow Specimen W/StrainGage Locations Identified

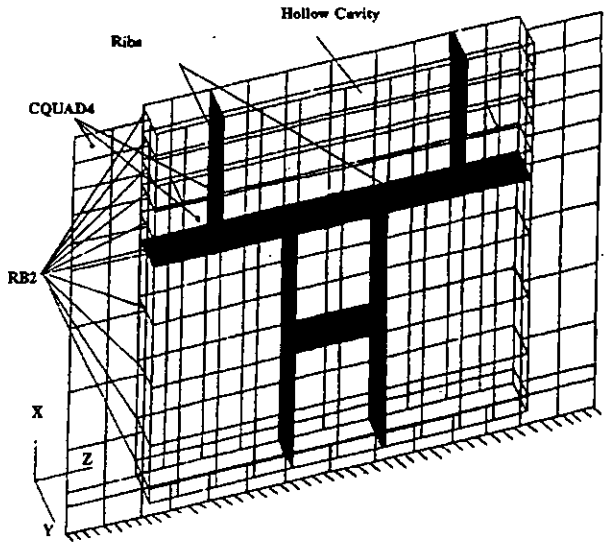

Figure 2: Finite Element Model For Hollow Specimens

Comparison between the NASTRAN and holography mode shapes are shown in Figure 3. The effect of placing an insert damper in the tip center cavity is studied extensively for the chordwise mode and to a limited extent on the first torsion mode.

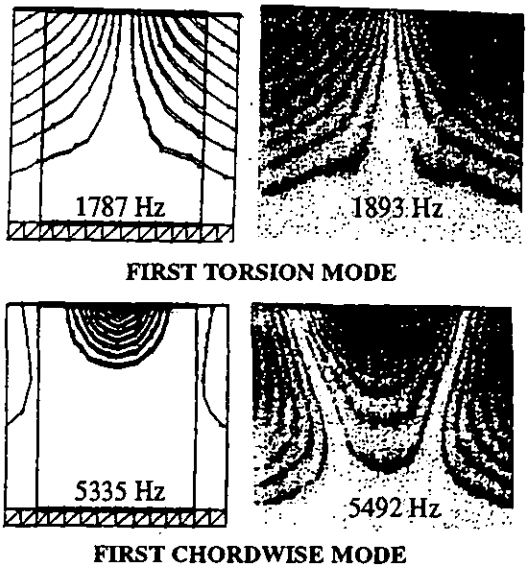

Figure 3: Comparison Between NASTRAN and Holographic Mode Shapes for Specimen PW12

2.2 Damper Design

Four damper configurations, shown in Figure 4, were designed to fit in the top center cavity, designated in the figure by the rectangular outline. In an ideal situation, validation of such

Downloaded from http://asmedigitalcollection.asme.org/GT/proceedings-pdf/GT1996/78767/V005T14A013/4464956/v005t14a013-96-gt-110.pdf by guest on 07 October 2022

concept is accomplished in a spin rig environment. However, the limited scope of the program dictated the damping investigation be conducted on a shaker table. This requirement has further limited the choices of how the damper is loaded against the hollow specimen. To compensate for the lack of the centrifugal loading, the dampers had to be spring-loaded inside the hollow cavity with varying degrees of preload representative of realistic blade running conditions. Furthermore, the damper configurations were selected to provide a range of contact locations to assess its effect on damping effectiveness for the different modes of interest.

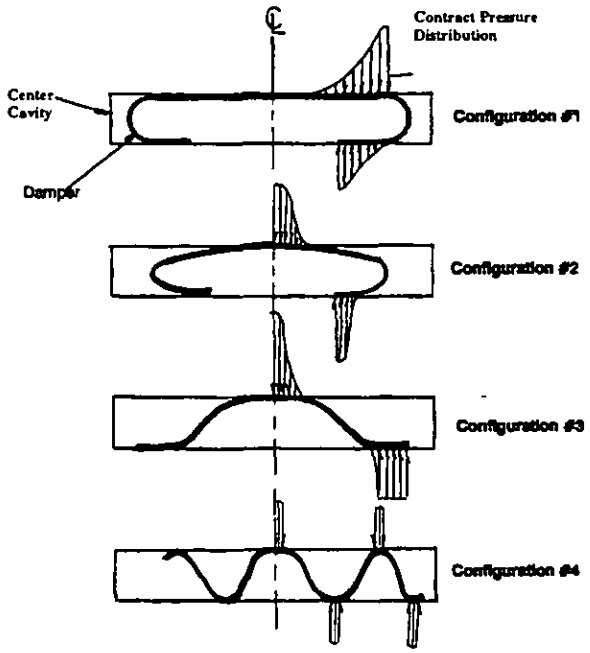

Figure 4: Damper Configurations

2.3 Damper Configurations and Preloads

The selected damper configurations are intended to provide different normal load distribution between the dampers and the interior walls of the cavity to study its effect on damping effectiveness. Each damper was hand formed and then heat treated to restore its elastic characteristics. Figure 5 is a photograph of the four damper configurations. Three sets of dampers were made for each configuration to provide a matrix of preloads. Later in the program, an additional stiffer damper was made for configuration 3 to expand its database. All dampers were made of 0.020 inch Waspaloy (AMS 5544) sheet stock except for the fourth damper of configuration 3 which was made of 0.027 inch sheet.

The damper preload for each configuration was determined by a static load test. Each damper is compressed from its initial undeformed height to the height correspondingto the inside dimension of the center cavity of 0.195 inch. A summary of the damper matrix preloads is shown in Table 1.

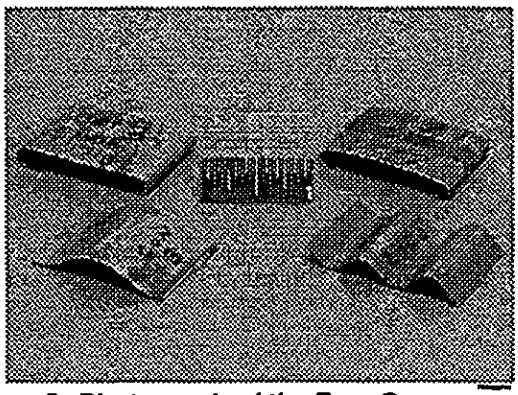

Figure 5: Photograph of the Four Damper Configurations

Table 1: Damper Matrix and Preloads

Damper Configuration	Set	Unloaded Dimension (Inch)	Loaded to 0.195" Dimension (lbs)
1	1	0.223 to 0.228	168
	2	0.210 to 0.215	90
	3	0.200 to 0.2.05	31
2	1	0.224 to 0.250	94
	2	0.232	56
	3	0.210 to 0.215	29
3	1	0.247 to .250	26
	2	0.230 to .235	19
	3	0.210 to .215	9
	4	0.250 (.027" thick)	50
4	1	0.202 to 0.209	177
	2	0.212	100
	3	0.219	50

2.4 Test Procedure

The damping characterization tests were accomplished using an electrodynamic shaker to provide the input excitation. The hollow specimen is secured between two fixture plates using the five bolt pattern illustrated in Figure 6. A block diagram showing the control loop and data acquisition system is presented in Figure 7. The strategy for determining the damper effectiveness was to measure the maximum dynamic stress on the hollow specimen in response to a servo-controlled input acceleration measured on the shaker plate. The frequency range of the input was chosen to include the specimen resonance of interest and was swept from low to high at a constant rate of 5 Hz/second. Different sweeps

Downloaded from http://asmedigitalcollection.asme.org/GT/proceedings-pdf/GT1996/78767/V005T14A013/4464956/v005t14a013-96-gt-110.pdf by guest on 07 October 2022

were made at input levels from 10 g's to 60 g's (single amplitude). The strain gages were conditioned using standard amplifiers and the measurements were made using the computer controlled acquisition system.

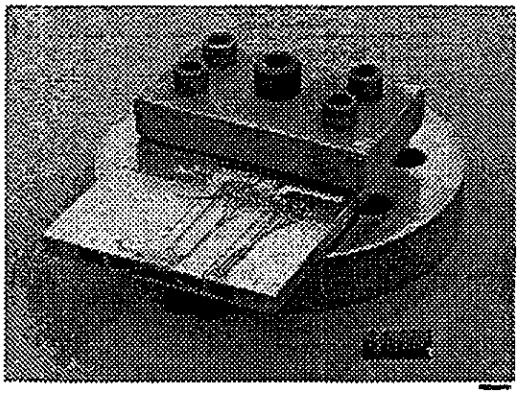

Figure 6: Specimen PW10 Instrumented and Mounted Between Fixture Plates

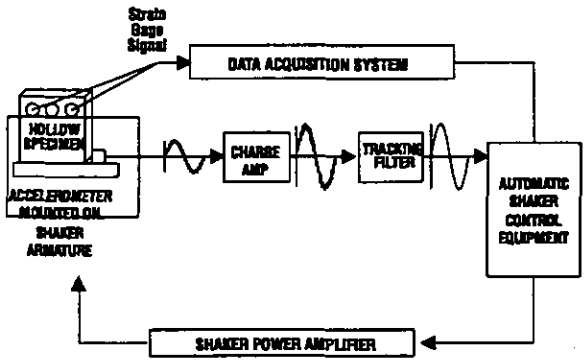

Figure 7: Block Diagram of Shaker Table Control Loop and Data Acquisition System

2.5 Damping Test Matrix

A test matrix of 211 cases were completed using three hollow specimens (PW10, PW11, and PW12) in conjunction with 12 dampers and 6 levels of input excitation. Repeatability tests were not included as part of the test matrix. Major emphasis was directed to the characterization of the chordwise bending mode. Nearly 80% of the effort was spent on the chordwise mode and 20% on the torsion mode. The damping test matrix for specimen PW10, for the chordwise mode, is shown in Table 2 as an example.

Table 2: Test Matrix for Specimen PW10

Specimen	Input G's	Configuration 1			Configuration 2			Configuration 3				Configuration 4			Baseline (undamped)	Mode
		Set 1	Set 2	Set 3	Set 1	Set 2	Set 3	Set 1	Set 2	Set 3	Set 4	Set 1	Set 2	Set 3		
PW10	10							✓	✓	✓	✓				✓	Chordwise
	20							✓	✓	✓	✓				✓	
	30	✓	✓	✓	✓	✓	✓	✓	✓	✓	✓	X	✓	✓	✓	
	40							✓	✓	✓	✓				✓	
	50							✓	✓	✓	✓				✓	
	60							✓	✓	✓	✓				✓	

With the exception of one damper (configuration 4, set 1) all dampers were tested in all three hollow specimens. However, configuration 3 was singled out to be the most effective and, therefore, received the largest coverage.

2.6 Damping Test Results

Damping test data were digitized and recorded on permanent electronic files. Each file contains frequency response spectrum data for all strain gages covering the mode of interest. Peak response amplitudes are determined from these response spectrum plots.

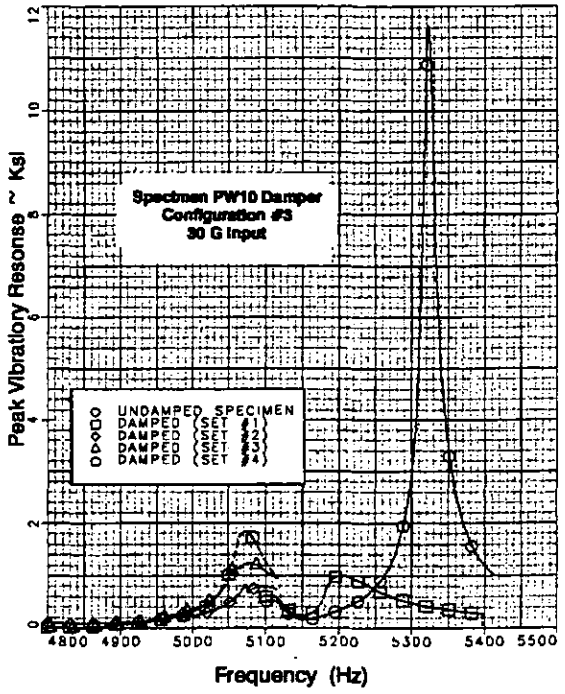

Figure 8: Frequency Response Spectrums for Undamped and Damped Specimen PW10– Chordwise Mode

Downloaded from http://asmedigitalcollection.asme.org/GT/proceedings-pdf/GT1996/78767/V005T14A013/4464956/v005t14a013-96-gt-110.pdf by guest on 07 October 2022

A typical response spectrum plot for the chordwise mode of specimen PW10, with and without internal dampers, subjected to 30G input is shown in Figure 8. Comparison of the damped and undamped responses indicate significant reduction in the peak amplitude response by an order of magnitude. The resonant frequency of the damped specimen has dropped from 5320 Hz to a range of 5075 to 5200 Hz. This 2 to 5% drop in frequency is attributed to the added damping and the additional damper mass.

All damper configurations were extremely effective in suppressing the vibratory response of the chordwise mode. Figure 9 compares the normalized response amplitudes for the different configurations. Configurations 2 and 3 provided the highest reduction in response. This may be attributed to the fact that both dampers have a large contact region in the area corresponding to the maximum vibratory amplitude. The effect of normal load on peak response exhibits the traditional characteristics of friction dampers, namely; the presence of an optimum normal load value that corresponds to the lowest peak response as shown in Figure 10..

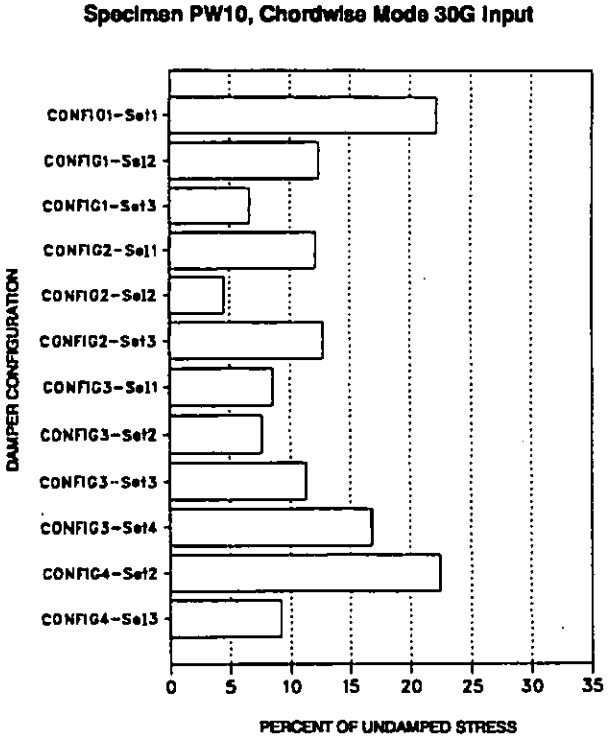

Figure 9: PW10 Damped Vibratory Responses as Percent of Undamped Stress Due to 30 G Input – Chordwise Mode

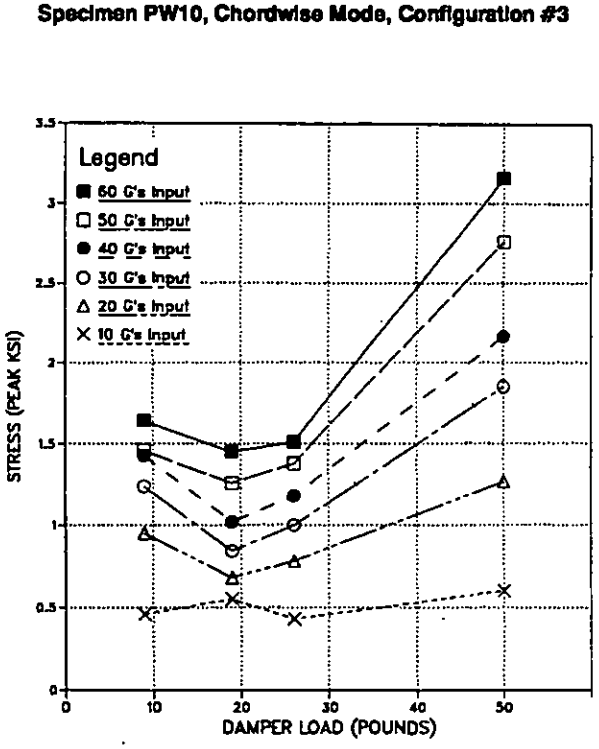

Figure 10: Effect of Damper Preload on Vibratory Stress Amplitudes for Specimen PW10 – Chordwise Mode

2.7 Correlations to Analytical Predictions

A micro–slip friction damping code based on the formulation described in Part I of this paper has been used to predict the damping effectiveness for selected damper configurations. The results of hollow specimen PW10 with damper configuration 3 were selected for the correlation. Figure 11 shows the predicted damper performance characteristics for three different coefficients of friction, 0.3, 0.5, and 0.7. Superposition of the test data, normalized by the normal load, on the predicted damper performance curve for a coefficient of friction of 0.3 is shown in Figure 12. Excellent correlations were achieved in the range where the data was collected. The collapse of the data in the region corresponding to slip on the damper performance curve indicate that the assumptions of Coulomb friction principles are valid under these test conditions.

Downloaded from http://asmedigitalcollection.asme.org/GT/proceedings-pdf/GT1996/78767/V005T14A013/4464956/v005t14a013-96-gt-110.pdf by guest on 07 October 2022

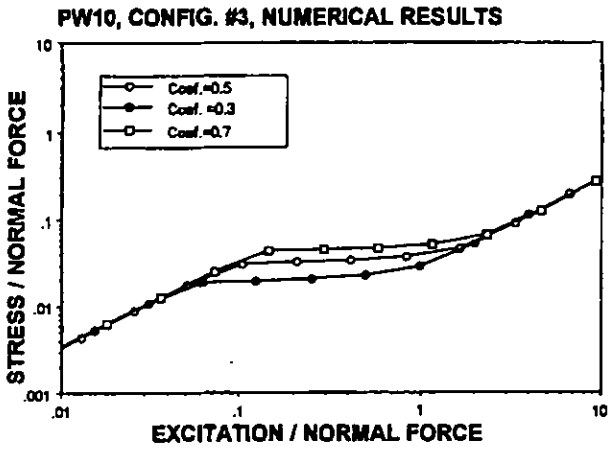

Figure 11: Predicted Damper Performance Using Micro–Slip Model

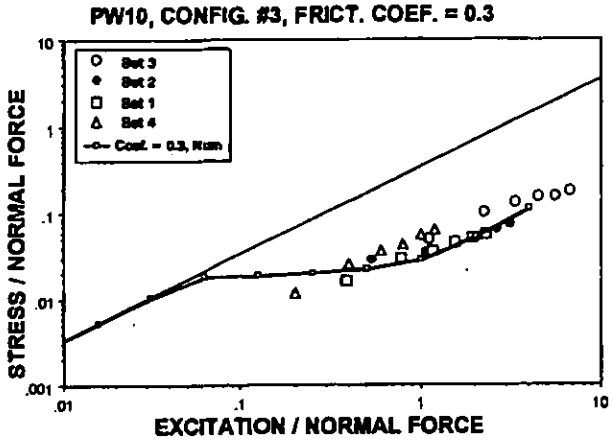

Figure 12: Correlation of Micro–Slip Model Predictions with Test Data

3. CONCLUSIONS

An experimental test program to investigate the effectiveness and viability of using internal friction dampers inside hollow airfoil–like specimens was conducted. In practice, the use of such approach would rely on the component of the centrifugal load to provide positive contact at all times and, therefore, avoid the potential loss of normal load due to wear or creep. The component of the centrifugal load, required to provide the normal load between the damper and the airfoil inside surface, is directly proportional to the Sine of the airfoil tilt angle measured from a radial plane perpendicular to the engine centerline. Due to the limited scope of the program, however, validation testing was conducted in a non–rotating environment with the intent of simulating the effect of normal loading via spring loaded dampers. The resulting conclusions should ,however, hold true for actual airfoil designs. The results of the test program indicate that internal dampers can provide an order of magnitude reduction in response when customized for the modes of interest. Positioning the damper in a location that correspond to maximum relative motion is required to maximize performance. While damper performance is generally optimized for a given mode, other modes that exhibit sufficient modal deflections in the vicinity of the damper can also benefit but to a lesser extent. For example, while damper configuration 3 has provided a 92% stress reduction for the chordwise bending mode the corresponding stress reduction for the torsion mode is in the range of 75%. The sensitivity of the response to the normal load was consistent with the classical characteristics of friction dampers. Optimum normal loads on the order of 20 lbs provided the lowest vibratory responses. However, because of the overwhelming effectiveness of the damper, all configurations have demonstrated significant response reductions for all preloads tested. As may be expected with all friction damper applications, damper and /or specimen contact surfaces will experience wear. Provisions to minimize wear, through application of selected coatings or increases in thicknesses in local areas, must be addressed in the design phase.

Finally, excellent agreement between the experimental test results and the analytical predictions of a micro–slip friction damping model has been illustrated. Both the trends of the normalized data and the correlation with the analytical model indicate that the use of the Coulomb friction principles is appropriate for the range of excitation levels and normal loads used in this investigation.

ACKNOWLEDGMENT

The investigation in this paper was funded by the Naval Air Warfare Center (NAWC) under Contract # N00140–91–C–2676 with Mr. Peter DiMarco as the contracting officer technical representative. The authors would like to thank W. Thomson, K. Nelson, and H. Powell of the Materials & Mechanics Engineering at Pratt and Whitney for assisting with the experimental test program.

REFERENCES

Griffin, J.H., 1980, "Friction Damping of Resonant Stresses in Gas Turbine Airfoils," *ASME Journal of Engineering for Power,* Vol. 102, pp.329–333.

Griffin,J.H., and Menq, C–H., 1991, "Friction Damping of Circular Motion and Its Implication to Vibration Control," *Journal of Vibration and Acoustics,* Vol. 113, pp.225–229.

Panossian, H.V., 1989, "Nonobstructive Impact Damping Applications for Cryogenic Environments," *Proceedings of Damping '89,* Sponsored by The Flight Dynamics Directorate at Wright Laboratory, WRDC–TR–89–3116, West Palm Beach, Florida.

Downloaded from http://asmedigitalcollection.asme.org/GT/proceedings-pdf/GT1996/78767/V005T14A013/4464956/v005t14a013-96-gt-110.pdf by guest on 07 October 2022